Modeling of Different Charge Transfer Modes in Upward Flashes Constrained by Simultaneously Measured Currents and Fields

Lixia He[1,2], Mohammad Azadifar[1,3], Quanxin Li[1,4], Marcos Rubinstein[3], Vladimir A. Rakov[5,6], Arturo Mediano[7], Davide Pavanello[8], Mario Paolone[1], Hongyan Xing[2] and Farhad Rachidi[1]

1 Institute of Electrical Engineering, Swiss Federal Institute of Technology (EPFL), 1015 Lausanne, Switzerland
2 Jiangsu Key Laboratory of Meteorological Observation and Information Processing, Nanjing University of Information Science and Technology, 210044 Nanjing, China
3 University of Applied Sciences of Western Switzerland (HES-SO), 1400 Yverdon-les-Bains, Switzerland
4 Dept. of Electrical Engineering, Wuhan University, Wuhan, China
5 Department of Electrical and Computer Engineering, University of Florida, Florida, USA
6 Institute of Applied Physics, Russian Academy of Sciences, Nizhny Novgorod, Russia
7 Dept. Electronics and Communication Engineering, University of Zaragoza, Zaragoza, Spain
8 University of Applied Sciences of Western Switzerland (HES-SO), 1950 Sion, Switzerland

***Abstract*— The purpose of the paper is to investigate charge transfer modes in upward lightning flashes by means of numerical simulation constrained by concurrent observations of electromagnetic fields and currents. In particular, we focus on different types of pulses occurring in upward negative flashes. The MTLE return stroke model is used to compute the electric fields associated with return strokes and mixed-mode pulses, while the M-component model of *Rakov et al.* (1995) is used to compute electric fields associated with M-components and M-component-type ICC pulses. The simulation results are constrained by experimental data consisting of simultaneous records of lightning currents and electric fields associated with upward flashes at the Säntis tower. The inferred velocities for M-component and M-component-type ICC pulses range from 2.0x10^7 m/s to 9.0x10^7 m/s, and the corresponding junction point heights range from 1.0 km to 2.0 km. The inferred pulse velocities for return strokes and mixed-mode pulses range from 1.3x10^8 m/s to 1.65x10^8 m/s. The inferred current attenuation constants of the MTLE model obtained in this study range from 0.3 km to 0.8 km, lower than the value of 2.0 km suggested in previous studies. The obtained results confirm the similarity of mixed-mode charge transfer to ground with return strokes on the one hand, and of the M-component-type ICC with classical M-components mode of charge transfer on the other hand.**

Keywords*— *Upward Negative Lightning; Current; Velocity; Electric field; Charge transfer mode; Return stroke; M-component; Mixed-mode pulses

I. Introduction

M-component is a transient process occurring during the continuing current of a cloud-to-ground lightning discharge and it has been studied for more than seven decades (e.g. [1]-[3]). M-components have distinct characteristics in terms of current peak, rise-time and the associated E-field waveform, significantly different from the mechanisms of charge transfer in return strokes [2].

Recently, *He et al.* [4] identified four types of pulses in upward negative flashes observed at the Säntis Tower, namely (i) return strokes, which occur after the extinction of the initial continuous current (ICC) and are preceded by a no-current interval, (ii) the so-called mixed-mode pulses [5], which are fast pulses superimposed on the ICC presumably due to the reactivation of a decayed branch or the connection of a newly-created channel to the ICC-carrying channel at low junction heights, with similar characteristics as return strokes [6], (iii) M-component mode pulses superimposed on the continuing current after some return strokes, and (iv) M-component-type ICC pulses, presumably associated with the reactivation of a decayed branch or the connection of a newly-created channel to the ICC-carrying channel at high junction heights [5].

In this study, we present simulation results for these four different types of pulses occurring in upward negative flashes. The simulations are compared with experimental data associated with upward flashes at the Säntis tower. The paper is organized as follows. Section II presents briefly the instrumentation at the Säntis tower and the considered dataset. The adopted computational models are presented in Section III. Model-predicted results and their comparison with experimental data are presented and discussed in Section IV. The paper ends with a summary and conclusions in Section V.

II. Instrumentation and Dataset

A. Lightning Current Measurement System

The Säntis Tower was instrumented in May 2010 with accurate and modern equipment to measure the lightning channel-base current and its time derivative. It contains two sets of measuring equipment, each including a Rogowski coil and a multi-gap B-Dot sensor mounted at two heights along the tower, 24 m and 82 m above ground level [7][8].

Financial supports from the Swiss National Science Foundation (Project No. 200021_147058) and the European Union's Horizon 2020 research and innovation programme (grant agreement. No 737033-LLR) are acknowledged. It is also supported by the Research Innovation Program of Colleges and Universities Postgraduates of Jiangsu Province, China (Grant No. KYZZ15_0245) and China Scholarship Council (CSC).

B. E-field Measurement System

The electric field measurement system is located 14.7 km away from the Säntis Tower, installed on the roof of a 25-m tall building in Herisau. It comprises a flat plate antenna and an analog integrator with an overall frequency bandwidth of 30 Hz to 2 MHz. The signal is digitized and recorded using a PCI 5122 National Instruments card with sampling rate of 5 MS/s and a time window of 4 s.

C. Dataset

The dataset is composed of simultaneous records of currents and E-field waveforms associated with pulses belonging to two upward negative flashes initiated from the Säntis Tower on August 4, 2016, at 23:52 and at 23:57 (Local Time). Two events were considered for each category of pulses, namely return strokes, mixed-mode pulses, M-components, and M-component-type ICC pulses.

It should be noted that the GPS system was not working properly during these two flashes. Therefore, we synchronized the current pulses and the associated electric field pulses manually by aligning the current peak and the associated field peak of the last return stroke for each flash. The error of the alignment was quantified to be in the order of a few microseconds [6].

III. Modeling

The vertical electric field is calculated assuming a vertical channel above a perfectly-conducting ground. The field expression is given by [9] [10],

$$E_z(d,t)=\frac{1}{2\pi\varepsilon_\circ}\int_{H_1(t)}^{H_2(t)}\frac{2z'^2-d^2}{R^5(z')}\int_{R/c}^{t} i(z',\tau-\frac{R}{c})d\tau dz' + \frac{1}{2\pi\varepsilon_\circ}\int_{H_1(t)}^{H_2(t)}\frac{2z'^2-d^2}{cR^4(z')} i\left(z',t-R(z')/c\right)dz' - \frac{1}{2\pi\varepsilon_\circ}\int_{H_1(t)}^{H_2(t)}\frac{d^2}{c^2R^3(z')}\frac{\partial i\left(z',t-R(z')/c\right)}{\partial t}dz' \quad (1)$$

in which $i(z',t)$ is the current as a function of z' and time t, c is the speed of light, d is the horizontal distance between the Säntis Tower and the observation point, which in our measurement setup is d=14.7 *km*, $R=(d^2+z'^2)^{1/2}$, $H_1(t)$ and $H_2(t)$ are the extremities of the radiating channel length. Based on the results of [11], an overall field enhancement factor of 2.0 due to the presence of the 124-m tower and the irregular mountainous terrain was taken into account in the simulations. The presence of the tower and possible transient processes excited in it were not considered in the simulations.

A. Current Distribution in Return Stroke and Mixed Charge Transfer Modes

As discussed in [6], the characteristics of mixed-mode pulses are very similar to those of return strokes. In this study, we use the same model for calculating the fields of return strokes and mixed mode pulses. The adopted model is the modified transmission line model with exponential current decay with height (MTLE) [12], [13], in which the current distribution is expressed as,

$$\begin{aligned} i(z',t) &= i_0(t-z'/v)e^{-z'/\lambda} \qquad z' \le vt \\ i(z',t) &= 0 \qquad z' > vt \end{aligned} \quad (2)$$

where v is the return stroke speed and λ is the attenuation constant.

B. Current Distribution in M-component and M-component-type ICC Pulse Charge Transfer Modes

M-components and M-component-type ICC pulses are modeled by a superposition of two current waves propagating without distortion: a downward incident current and an upward current reflected at the bottom of the lightning channel ([2] and [14]). The distribution of the M-component mode current along the ICC or continuing-current-carrying channel is expressed as follows.

$$\begin{aligned} &\text{if} \quad t < h_m/v_m, \\ &i(z',t) = i(h_m, t-(h_m-z')/v_m) \\ &\text{if} \quad t \ge h_m/v_m, \\ &i(z',t) = i(h_m, t-(h_m-z')/v_m) + i(h_m, t-(h_m+z')/v_m)\,\rho_g \end{aligned} \quad (3)$$

where v_m is the velocity of the M-components/M-component-type ICC pulse current wave, h_m is the height of the junction point between the leader and the ICC/CC carrying channel and ρ_g is the reflection coefficient at the ground.

IV. Simulation Results and Comparison with Experimental Data

Figs. 1 to 8 present the simulation results (red curves) and measured data (blue curves). For each pulse, the measured current was represented analytically by the sum of two Heidler's functions with parameters evaluated using a genetic algorithm [15]. The parameters of the models, namely v and λ for return strokes and mixed-mode pulses, and v_m, h_m, and ρ_g for M-components and M-component-type ICC pulses, were adjusted to match the simulation results with the experimental data.

A. Return Strokes and Mixed-Mode Pulses

Fig. 1 (b) to Fig. 4 (b) present the simulation results for two return strokes and two mixed-mode pulses. From these figures, one can see that the calculated fields for both return strokes and mixed-mode pulses are in excellent agreement with the measured waveforms. For the simulations presented in Fig. 1 (b) to Fig. 4 (b), the parameters v and λ (see Table I) were adjusted to obtain a good qualitative fit with the measured fields. It should be noted that the waveforms of Fig. 2 are affected by some oscillations whose origin is currently unknown.

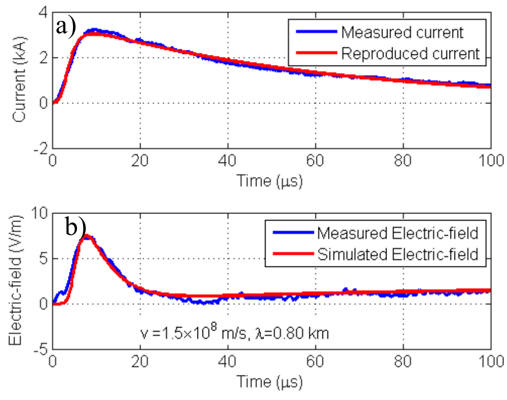

Fig. 1 Current (a) and electric field (b) waveforms produced by a mixed-mode pulse (MM1) of a flash that occurred on August 4, 2016 at 23:57 local time.

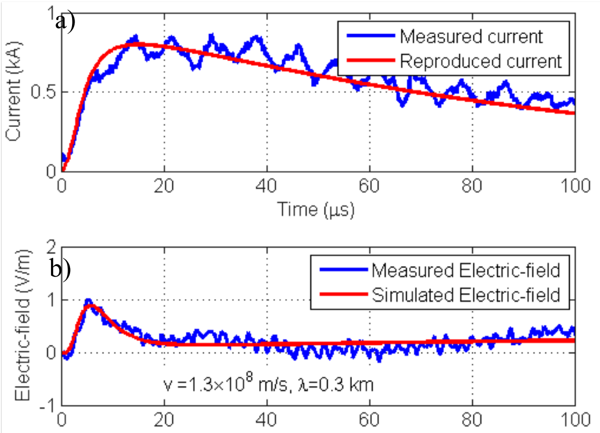

Fig. 2 Current (a) and electric field (b) waveforms produced by a mixed-mode pulse (MM2) of the flash that occurred on August 4, 2016 at 23:57 local time.

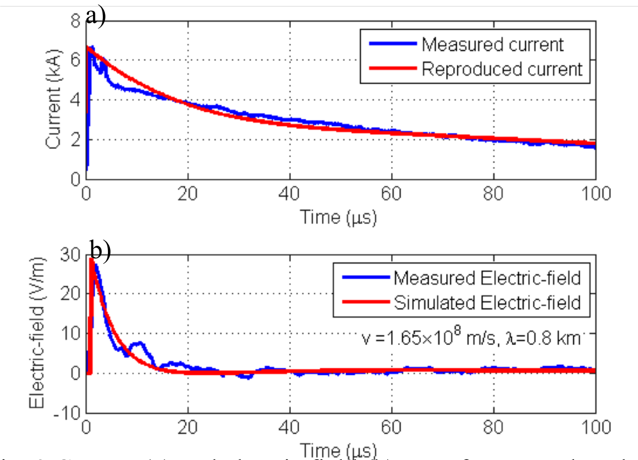

Fig. 3 Current (a) and electric field (b) waveforms produced by a return stroke (RS1) of a flash that occurred on August 4, 2016 at 23:52 local time.

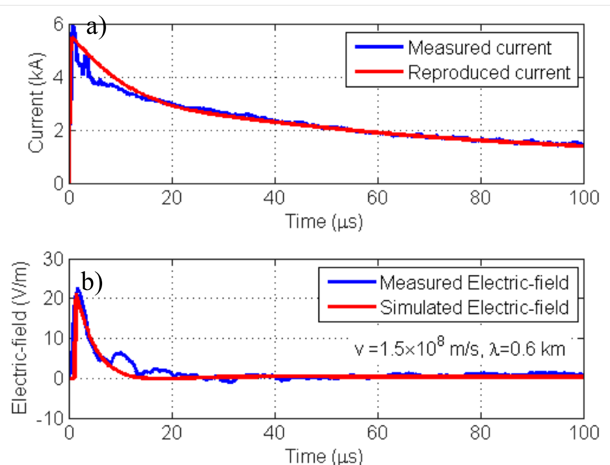

Fig. 4 Current (a) and electric field (b) waveforms produced by a return stroke (RS2) of the flash that occurred on August 4, 2016 at 23:52 local time.

The model parameters providing the best match to measured fields for each pulse are given in Table 1. The velocities of the four pulses range from 1.3x10^8 m/s to 1.65x10^8 m/s, which is in the range of the experimentally-observed return stroke speeds (e.g., [16] and [17]). However, the exponential attenuation height constants λ for the four pulses are from 0.3 km to 0.8 km, lower than the value of 2.0 km suggested in [18] and [12].

The good agreement between the vertical electric fields predicted by the MTLE return stroke model and the measured field waveforms for mixed-mode pulses supports the hypothesis that the charge transfer mode resulting in mixed-mode pulses is similar to that of return strokes.

B. M-Components and M-Component-Type ICC Pulses

Fig. 5 (b) to Fig. 8 (b) present the simulation results for M-components and M-component-type ICC pulses, which are believed to be manifestations of the same mode of charge transfer to ground. Model parameters (v_m, h_m, and ρ_g) providing the best match between computed and measured fields are given in Fig. 5 (b) to Fig. 8 (b).

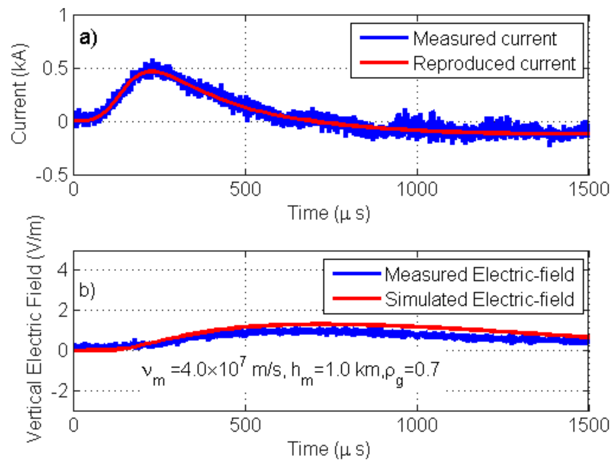

Fig. 5 Current (a) and electric field (b) waveforms produced by an M-component (MC1) of the flash that occurred on August 4, 2016 at 23:52 local time.

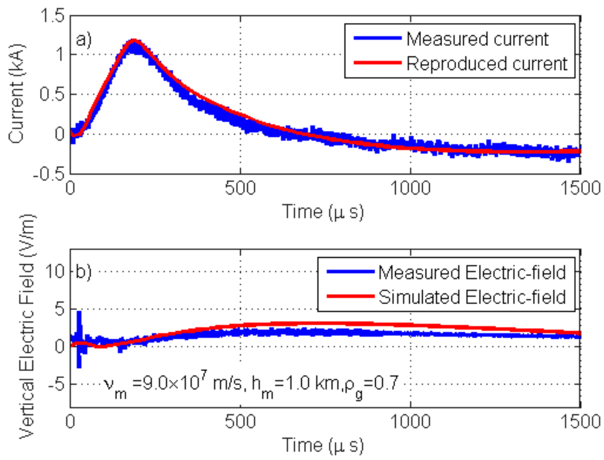

Fig. 6 Current (a) and electric field (b) waveforms produced by an M-component (MC2) of the flash that occurred at 23:57 on August 4, 2016 local time.

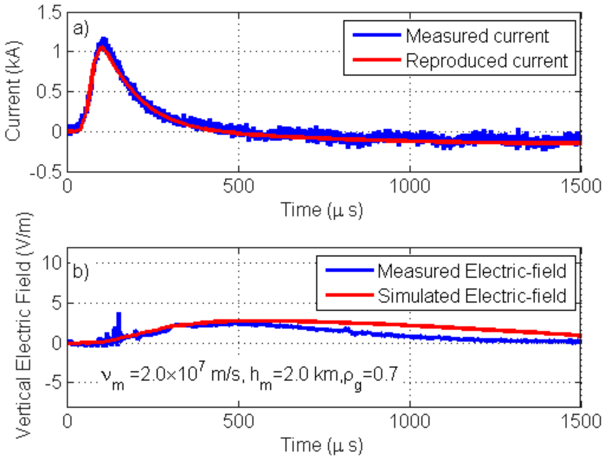

Fig. 7 Current (a) and electric field (b) waveforms produced by an M-component-type ICC pulse (MICC1) of the flash that occurred on August 4, 2016 at 23:52 local time.

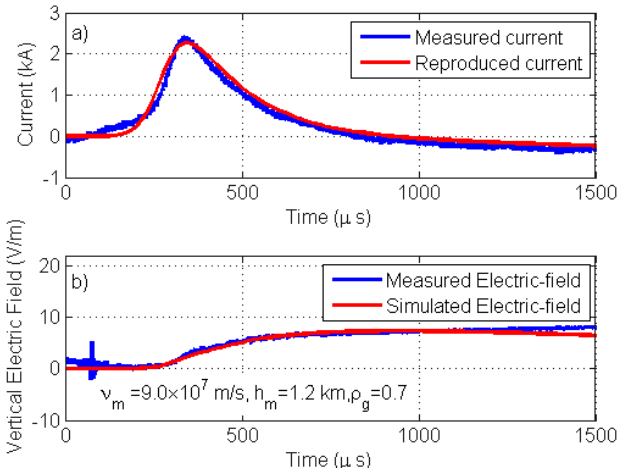

Fig. 8 Current (a) and electric field (b) waveforms produced by an M-component-type ICC pulse (MICC2) of the flash that occurred on August 4, 2016 at 23:52 local time.

From Fig. 5 (b) and Fig. 6 (b), one can see that the simulated fields for M-component pulses are in good agreement with the corresponding measured fields. Although there are slight deviations in the trailing edge of the waveforms (after about 650 µs for MICC1 and after 1250 µs for MICC2, see Fig. 7 (b) and Fig. 8 (b)), the simulated fields and the corresponding measured waveforms for M-component-type ICC pulses are also in good agreement with each other.

The model parameters providing the best match to measured fields for each pulse are shown in Table 1. The propagation speeds for the four pulses range from 2.0x10^7 m/s to 9.0x10^7 m/s, which are in the range of speeds expected for M-components in [2] and [19]. The junction point heights for M-components and M-component-type ICC pulses range from 1.0 km to 2.0 km which are consistent with the study presented in [5]. Note that the value of the ground reflection coefficient (0.7) is smaller than the value suggested by *Rakov et al*. [2]. However, it can be justified by the fact that upward-moving current pulses along the tower suffer attenuation that can be represented by an equivalent, lower value for the ground reflection coefficient [20].

Table 1 Parameters derived from matching simulated and measured field

Event ID	$v/(\times 10^8 m/s)$	H/km	λ/km	Event ID	$v_m/(\times 10^7 m/s)$	h_m/km	ρ_g
MM1	1.50	8.00	0.80	MC1	4.00	1.00	0.70
MM2	1.30	8.00	0.30	MC2	9.00	1.00	0.70
RS1	1.65	8.00	0.80	MICC1	2.00	2.00	0.70
RS2	1.50	8.00	0.60	MICC2	9.00	1.20	0.70

The good agreement between the vertical electric fields predicted by the M-component model and the measured field waveforms for M-component-type ICC pulses supports the assumption that their charge transfer mode is similar to that of M-components.

V. CONCLUSIONS

In this paper, we presented simulation results for different types of pulses occurring in upward negative flashes. The MTLE return stroke model was used to compute electric fields associated with return strokes and mixed-mode pulses, while the M-component model of *Rakov et al.* [2] was used to compute electric fields associated with M-components and M-component-type ICC pulses. The simulation results were compared with experimental data consisting of simultaneous records of lightning currents and electric fields associated with upward flashes at the Säntis Tower.

The inferred velocities for M-components and M-component-type ICC pulses range from 2.0x10^7 m/s to 9.0x10^7 m/s, and the corresponding junction point heights range from 1.0 km to 2.0 km. The inferred pulse velocities for return strokes and mixed-mode pulses range from 1.3x10^8 m/s to 1.65x10^8 m/s. The inferred current attenuation constants of the MTLE model obtained in this study range from 0.3 km to 0.8 km, lower than the value of 2.0 km suggested for return strokes in previous studies.

The obtained results support the assumption that the mode of charge transfer to ground giving rise to mixed-mode pulses is similar to that of return strokes. The results are also in support of generally assumed similarity between M-component-type ICC pulses and classical M-components.

REFERENCES

[1] Malan, D., and H. Collens (1937), Progressive lightning. III. The fine structure of return lightning strokes, Proc.R.Soc.Lond.A Math.Phys.Sci., 175-203.

[2] Rakov, V. A., R. Thottappillil, M. A. Uman, and P. P. Barker (1995), Mechanism of the lightning M component, J. Geophys. Res., 100, 25,701-725,710.

[3] Campos, L. Z., M. M. Saba, O. Pinto, and M. G. Ballarotti (2007), Waveshapes of continuing currents and properties of M-components in natural negative cloud-to-ground lightning from high-speed video observations, Atmos. Res., 84(4), 302-310.

[4] L. He, M. Azadifar, F. Rachidi, M. Rubinstein,V.A.Rakov,V. Cooray, D. Pavanello, H. Xing, An Analysis of Current and Electric Field Pulses Associated with Upward Negative Lightning Flashes Initiated from Tall Structures , submitted to the J.Geophys.Res., 2017.

[5] Zhou, H., V. A. Rakov, G. Diendorfer, R. Thottappillil, H. Pichler, and M. Mair (2015), A study of different modes of charge transfer to ground in upward lightning, J. Atmos. Terr. Phys., 125–126, 38-49, doi: http://dx.doi.org/10.1016/j.jastp.2015.02.008.

[6] Azadifar, M., F. Rachidi, M. Rubinstein, V. A. Rakov, M. Paolone, D. Pavanello, and S. Metz (2016), Fast initial continuous current pulses versus return stroke pulses in tower-initiated lightning, J.Geophys.Res.Atoms., 121(11), 6425-6434, doi: 10.1002/2016jd024900.

[7] Azadifar, M., M. Paolone, D. Pavanello, F. Rachidi, V. Rakov, C. Romero, and M. Rubinstein (2014), An update on the charaterictics of positive flashes recorded on the Säntis Tower, paper presented at 2014 International Conference on Lightning Protection (ICLP), IEEE.

[8] Romero, C., A. Mediano, A. Rubinstein, F. Rachidi, M. Rubinstein, M. Paolone, P. Zweiacker, N. Mora, D. Pavanello, and B. Daout (2010), Measurement of lightning currents using a combination of Rogowski coils and B-Dot sensors, paper presented at Lightning Protection (ICLP), 2010 30th International Conference on, IEEE.

[9] Uman, M. A., D. K. McLain, and E. P. Krider (1975), The electromagnetic radiation from a finite antenna, Am. J. Phys., 43(1), 33-38

[10] Rubinstein, M., and M. A. Uman (1989), Methods for calculating the electromagnetic fields from a known source distribution: Application to lightning, IEEE Trans. Electromagn. Compat., 31(2), 183-189.

[11] Li, D., M. Azadifar, F. Rachidi, M. Rubinstein, M. Paolone, D. Pavanello, S. Metz, Q. Zhang, and Z. Wang (2016), On lightning electromagnetic field propagation along an irregular terrain, IEEE Trans. Electromagn. Compat., 58(1), 161-171.

[12] Nucci, C. A., C. Mazzetti, F. Rachidi, and M. Ianoz (1988), On lightning return stroke models for LEMP calculations, paper presented at 19th International Conference on lightning protection(ICLP).

[13] Rachidi, F., and C. Nucci (1990), On the Master, Uman, Lin, Standler and the modified transmission line lightning return stroke current models, J.Geophys.Res.Atoms., 95(D12), 20389-20393.

[14] Rakov, V. A., D. E. Crawford, K. J. Rambo, G. H. Schnetzer, M. A. Uman, and R. Thottappillil (2001), M ‐ component mode of charge transfer to ground in lightning discharges, J.Geophys.Res.Atoms., 106(D19), 22817-22831.

[15] Bermudez, J., C. Pena-Reyes, F. Rachidi, and F. Heidler (2002), Use of genetic algorithms to extract primary lightning current parameters, EMC Eur. Int. Symp. Electromagn. Compat. Sorrento, Italy, 2002.

[16] Idone, V. P., and R. E. Orville (1982), Lightning return stroke velocities in the Thunderstorm Research International Program (TRIP), J.Geophys.Res. Oceans, 87(C7), 4903-4916.

[17] Rakov, V. A. (2007), Lightning return stroke speed, J. Lightning Res, 1, 80-89.

[18] Nucci, C., and F. Rachidi (1989), Experimental validation of a modification to the Transmission Line model for LEMP calculation, paper presented at 8th Symposium and Technical Exhibition on Electromagnetic Compatibility.

[19] Jordan, D. M., V. P. Idone, R. E. Orville, V. A. Rakov, and M. A. Uman (1995), Luminosity characteristics of lightning M components, J.Geophys.Res.Atoms., 100(D12), 25695-25700.

[20] Shoory, A., F. Vega, P. Yutthagowith, F. Rachidi, M. Rubinstein, Y. Baba, V. A. Rakov, K. Sheshyekani, and A. Ametani (2012), On the Mechanism of Current Pulse Propagation Along Conical Structures: Application to Tall Towers Struck by Lightning, IEEE Trans. Electromagn. Compat., 54(2), 332-342, doi: 10.1109/temc.2011.2160068.